# ON THE STABILITY OF COMPRESSIBLE BOUNDARY LAYERS WITH HIGH MACH NUMBERS : PART I -EFFECT OF FREE STREAM VELOCITY.

***Ayman A. Al-Maaitah and Monther A. Al-Farah Nimri***

Department of Mechanical Engineering, Mu'tah University P. O. Box 7
Mu'tah , Al-Karak- Jordan

**ABSTRACT**

Controlling the supersonic laminar boundary layer stability by induced pressure gradient is investigated. Various Mach numbers, Reynolds numbers, wave frequencies, and wave angles are considered. It is shown that neglecting the non-similar effect of the boundary-layer (as sometimes practised in literature) generates a considerable inaccuracy of the results. Different classes of pressure gradient are analyzed. The calculations show that accelerated flow stabilizes the boundary layer while retarded flow disabilities it. The most unstable second mode is two dimensional even when pressure gradient is induced. Simply retarded flows are more stable for low frequencies than for high frequencies.

***Keywords:*** Supersonic boundary Layer, Stability, Pressure gradient, Free stream velocity, Laminar flow control

**NOMENCLATURE**

- $x$ streamwise coordinate parallel to surface.
- $y$ streamwise coordinate perpendicular to x.
- $\rho$ fluid density.
- $\mu$ fluid viscosity.
- $u$ velocity component in x-direction.
- $v$ velocity component in y-direction.
- $z$ velocity component in z-direction.
- $p$ flow pressure.
- $Re$ flow Reynolds number based on L*
- $L^*$ Characteristic length
- $R$ local Reynolds number based on displacement thickness
- $\gamma$ gas constant ($C_p/C_v$)
- $T$ temperature.
- $Pr$ Prandtl number.
- $M$ Mach number
- $C_p$ gas specific heat at constant pressure.
- $C_v$ gas specific heat at constant volume.
- $U_e$ non-dimensional velocity at edge of boundary layer.
- $\xi(x)$ levy-lees variable corresponding to x.
- $\eta$ levy-lees variable corresponding to x and y
- $\beta_0$ similarity constant corresponding to pressure gradient.
- $T_e$ non-dimensional temperature at edge of boundary-layer.
- $\alpha$ disturbance wave number in x-direction.
- $\beta$ disturbance wave number in z-direction.
- $\omega$ disturbance frequency.
- $\Psi$ wave angle.
- $\zeta_i$ disturbance mode shape.

**Scripts**

- $*$ physical (dimensional) quantity.
- $\infty$ free stream quantity.
- $i$ imaginary part.
- $r$ real part.
- $b$ basic flow quantity.

## INTRODUCTION

Ever since Prandtl has founded the concept of boundary -layer, scientists attempt to investigate methods of its control. In fact some of Prandtl's work at the beginning of this century describes several

experiments in which the boundary layer was controlled [1].In doing so, one aims to affect the whole flow in a described direction by influencing the structure of the boundary-layer. Out of the same stream a subject termed Laminar Flow Control (LFC) emerged in the sixties [2] Unlike Boundary-Layer Control, LFC is concerned with maintaining laminar flow over a body or a surface for the longest distance possible by delaying transition to turbulent flow. It is well established that transition from laminar to turbulent flow is preceded by the onset of instability waves [3]. Actually these instability waves were theoretically demonstrated by Tollmien [1] half a century ago and were later called the Tollmien-Shlichting (T-S) waves.

Later in the seventies, and due to the energy crisis, more emphasis was placed on LFC, especially since turbulent skin friction is of the order of 50% of the total cruise drag [4] of airplanes. The portion of the turbulent friction drag gets higher for other hydraulic applications. For example, for a vehicle having a moderate Reynolds number, applications of laminar flow control provides a lucrative increase in fuel efficiency [5]. The principal of LFC proved to be a very important practical concept for engineers, especially since its feasibility was improved due to many factors that include production of advanced high strength materials, modern fabrication and manufacturing techniques, and super-critical airfoils [6].

Recently the increasing interest in supersonic aircraft is provoking more investigation of the stability of compressible boundary-layer. By delaying transition to turbulent flow, LFC can lead to considerable increment in the range of supersonic missiles and rockets and in the speed maneuverability, and control of aircraft [7]. Moreover, LFC gained great attention lately due to its role in the design of the national areo-space plane (NASP). For the later application, in particular, the knowledge of the exact location of transition and controlling it is crucial for proper aero-thermal design. The three most used techniques in LFC are cooling or heating, pressure gradient, and wall suction. Good reviews of these techniques and their application in incompressible flows can be found in References 8 and 9.

Although the same techniques used for the laminar control of subsonic flows can be used for supersonic flows, the problem of supersonic flow control is much more complicated. For a comprehensive review of the stability of compressible boundary layers we refer the reader to the article of Mack [10] and Maaitah [15]. In addition, Malik [12] also attempted to calculate the effect of pressure gradient on the stability of supersonic boundary layer. His results, however, are questionable since his assumption of self-similar velocity profile is not valid for the Prandtl numbers he used.

All of the previously mentioned works are restricted to a single Mach number . An understanding of the physics of the flow and the mechanism which LFC techniques affect the stability of the flow is still lacking for supersonic boundary layers. In this paper we present a detailed and comprehensive investigation of the effect of pressure gradient, on the stability of supersonic boundary layers. Wide ranges of Mach numbers, frequencies, Reynolds numbers, and wave angles are considered. Furthermore, we present results for non-similar and self-similar boundary-layers.

## PROBLEM FORMULATION

### Mean flow

We consider the two-dimensional compressible flow over a flat plate with streamwise variation of the edge velocity. This is a basic Boundary-layer problem for many geometries [1]. The basic-flow field is governed by the compressible two-dimensional boundary layer equations. For a perfect gas the governing equations in a non-dimensional form is as follows:

X-momentum equation:

$$\rho u \frac{\partial u}{\partial x} + \rho v \frac{\partial u}{\partial y} = -\frac{dp}{dx} + \frac{1}{Re} \frac{\partial}{\partial y}\left(\mu \frac{\partial u}{\partial y}\right) \qquad (1)$$

Continuity equation:

$$\frac{\partial(\rho u)}{\partial x}+\frac{\partial(\rho v)}{\partial y}=0 \qquad (2)$$

Energy equation:

$$\rho u\frac{\partial T}{\partial x}+\rho v\frac{\partial T}{\partial y}=(\gamma-1)M_\infty u\frac{dp}{dx}+\frac{1}{Re\,Pr}\frac{\partial}{\partial y}\left(k\frac{\partial T}{\partial y}\right)+\frac{(\gamma-1)}{Re}M_\infty^2\mu\left(\frac{\partial u}{\partial y}\right)^2 \qquad (3)$$

where x is the streamwise direction and y is the direction normal to the flat plate. Velocities are normalized with respect to the free stream velocity $U^*_\infty$, lengths are normalized with respect to a reference length $L^*$, and the temperature, viscosity, and thermal conductivity coefficients are normalized with respect to their free-stream value $T^*_\infty$, $\mu^*_\infty$, and, $K^*_\infty$, respectively. Here,

$$Re=\frac{U^*_\infty L^*\rho^*}{\mu^*_\infty},\quad Pr=\frac{\mu^*_\infty C^*_p}{k^*_\infty},\quad \text{and}\quad \gamma=\frac{C^*_p}{C^*_v} \qquad (4)$$

Where $C^*_p$ and $C^*_v$ are the gas specific heat coefficients at constant pressure and volume, respectively. For a perfect gas the non-dimensional equation of state has the form

$$\rho T=\rho_e T_e \qquad (5)$$

Where $\rho_e$ and $T_e$ are the density and the temperature at the edge of the boundary layer, respectively. Away from the wall the boundary conditions are

$$u\to U_e,\ \text{and}\ T\to T_e\ \text{as}\ y\to\infty \qquad (6)$$

Where $U_e$ and $T_e$ can in general be found by solving the compressible Euler's equations.

The boundary conditions at the wall, however, are different for the different flow conditions. For flow with pressure gradient over an adiabatic wall the temperature gradient at the wall vanishes, that is:

$$\frac{\partial T}{\partial y}=0\ \text{at}\ y=0 \qquad (7)$$

It is convenient to re-formulate the problem using the Levy-Lees variables[1], defined as:

$$\xi(x)=\int_0^x \rho_e\mu_e U_e dx \qquad (8)$$

and

$$\eta,x,y=\sqrt{\frac{Re\,U_e}{2\xi}}\int_0^y \rho dy \qquad (9)$$

then Equations 1 to 3 will be transformed into the form:

$$(cf_{\eta\eta})_\eta+ff_{\eta\eta}+\beta_0[(\rho_e/\rho)(f_\eta)^2=2\xi(f f_{\eta}f_\xi-f f_\eta f_\xi) \qquad (10)$$

$$(a_1Q_\eta+a_2 f_\eta ff_{\eta\eta})_\eta fQ_\eta=2\xi(\eta f\, Q_\xi\, Q_\eta f_\xi \qquad (11)$$

Where

$$u=U_e f_\eta \qquad (12)$$

$$v=\frac{-1}{\rho\sqrt{Re}}\left[\frac{R_e U_e\mu_e}{\sqrt{2\xi}}(f+2\xi f_\xi)-\eta_x f_\xi\sqrt{2\xi}\right] \qquad (13)$$

$$c=\frac{\rho\mu}{\rho_e\mu_e} \qquad (14\text{-a})$$

$$\beta_0=(2\xi/U_e)\frac{dU_e}{d\xi} \qquad (14\text{-b})$$

$$Q=t/t_e \qquad (14\text{-c})$$

$$a_1=c/pr \qquad (14\text{-d})$$

and

$$a_2=c\frac{U_e^2}{T_e}\left(1-\frac{1}{Pr}\right) \qquad (14\text{-e})$$

The pressure gradient at the edge of the boundary layer occurs due to the variation of $U_e$ with x. In general the pressure gradient can be controlled by changing the shape of the rigid body or by placing a surface above the boundary layer. The variance of $U_e$ with respect to x is represented by $\beta_0$ in equation 10.

Malik [12] has assumed a self-similar solution for compressible flows with constant $\beta_0$. Although this assumption is valid for compressible flows where the energy equation is de-coupled from the momentum equation, it is not valid for compressible flows with Pr unequal to unity. For non-zero, $\beta_0$, $U_e$ varies with $\xi$ as shown by Equation 14-b. Consequently this would make the term $a_1$ in Equation 11 a function of $\xi$ for a non-unity Prandtl number which forces Equation 11 to have both $\xi$ and $\eta$ as variables. Hence the self-similar solution is not valid.

In the present work the non-similar boundary layer equations are used for various ranges and types of pressure gradient. For a constant $\beta_0 \geq 0$ and <1 one

can show that the dependence of $U_e$ on x is governed by the relation:

$$\int_{u_0}^{U_e} \frac{U_e^{\left(\frac{2-2\beta_o}{\beta_o}\right)}}{\rho_e \mu_e} dU_e = C_o x \qquad (15\text{-a})$$

Where $C_o$ is a constant which depends on the down-stream velocity and $\beta_o$ for $C_o=1$. When $\beta_o$ is positive the flow is accelerated and when $\beta_o$ is negative the flow is retarded.

Other types of pressure gradient considered in the present work are the simply accelerated flows where

$$U_e=1+x \qquad (15\text{-b})$$

and the simply retarded flows where

$$U_e=1-x \qquad (15\text{-c})$$

After defining $U_e$ and $\beta_o$ from Equation 15 one can calculate c, $a_1$, and $a_2$. Furthermore, Equations 12 and 13 are subjected to the following boundary conditions:

$f = f_\eta = 0$, and $Q = 0_\eta = 0$ for

$\eta=0$ (16-a)

$Q\to 1$ and $f'\to 1$ as $\eta\to\infty$ (16-b)

$f(\xi_0,\eta)=f_0$ (17)

Where $f_0$ corresponds to Blasuis profile.

Hence for a certain Prandtl number, equations 10,14,16 and17 are solved using central differencing in the transverse direction and three-point backward differencing in the streamwise direction.

The dependence of the viscosity on the temperature is given by:

$$\mu^* = \begin{cases} \dfrac{1.458\times10^{-5}\,T^{*2/3}}{T^*+110.4} & \text{if} \quad T^* \geq 110.4K \\ 6.9387\times10^{-7}\,T^* & \text{if} \quad T^* \leq 110.4K \end{cases} \qquad (18)$$

Where T* is in K and $\mu^*$ is $N.s/m^2$.

In the present work it is sometimes referred to the wind tunnel temperature, which is defined to be the free stream temperature based on the stagnation temperature of 311 K. If the resulting $T^*_\infty$ is less than 50 K it is set equal to 50 K. The adiabatic wall temperature is taken to be the recovery temperature $T_r$ given by [1],

$$T_r = T_\infty\left(1+\sqrt{Pr}\,\frac{\gamma-1}{2}M_\infty^2\right) \qquad (19)$$

## STABILITY ANALYSIS

We consider the linear quasi-parallel 3D compressible stability of the calculated 2D mean flow field, on it we superimpose a small disturbance and obtain the total flow quantities in the form

$$\hat{q}(x,y,z,t) = q_b(y)+q(x,y,z,t) \qquad (20)$$

where q stands for u, v, w, ρ,p, μ and T. The hat stands for the total-flow quantities. Substituting Equation 20 into the compressible Navier-Stokes equation, and linearizing with respect to q, we obtain the disturbance equations:

$$\frac{\partial\rho}{\partial t}+\rho_b\frac{\partial u}{\partial x}+u_b\frac{\partial\rho}{\partial x}+\frac{\partial}{\partial y}(\rho_b v)+\rho_b\frac{\partial w}{\partial z}=0 \qquad (21)$$

$$\rho_b\left(\frac{\partial u}{\partial t}+u_b\frac{\partial u}{\partial x}+v\frac{du_b}{\partial y}\right)=-\frac{\partial p}{\partial x}+\frac{1}{R}\left\{\mu_b\frac{\partial}{x}\left(r\frac{\partial u}{\partial x}+m\frac{\partial v}{\partial y}+m\frac{\partial w}{\partial z}\right)+\right.$$
$$\left.\frac{\partial}{\partial y}\left[\mu_b\left(\frac{\partial u}{\partial y}+\frac{\partial v}{\partial x}\right)+\mu\frac{du_b}{dy}\right]+\mu_b\frac{\partial}{\partial z}\left(\frac{\partial w}{\partial x}+\frac{\partial u}{\partial z}\right)\right\} \qquad (22)$$

$$\rho_b\left(\frac{\partial v}{\partial t}+u_b\frac{\partial v}{\partial x}\right)=-\frac{\partial p}{\partial y}+\frac{1}{R}\left\{\frac{\partial}{\partial x}\left[\mu_b\left(\frac{\partial u}{\partial y}+\frac{\partial v}{\partial x}\right)+\mu\frac{du_b}{dy}\right]\right.$$
$$\left.+\frac{\partial}{\partial y}\left[\mu_b\left(m\frac{\partial u}{\partial x}+r\frac{\partial v}{\partial y}+m\frac{\partial w}{\partial z}\right)\right]+\mu_b\frac{\partial}{\partial z}\left(\frac{\partial v}{\partial z}+\frac{\partial w}{\partial y}\right)\right\} \qquad (23)$$

$$\rho_b\left(\frac{\partial w}{\partial t}+u_b\frac{\partial w}{\partial x}\right)=-\frac{\partial p}{\partial z}+\frac{1}{R}\left\{\mu_b\frac{\partial}{\partial x}\left(\frac{\partial w}{\partial x}+\frac{\partial u}{\partial z}\right)\right.$$
$$\left.+\frac{\partial}{\partial y}\left[\mu_b\left(\frac{\partial v}{\partial z}+\frac{\partial w}{\partial y}\right)\right]+\mu_b\frac{\partial}{\partial z}\left(m\frac{\partial u}{\partial x}+m\frac{\partial v}{\partial y}+r\frac{\partial w}{\partial z}\right)\right\} \qquad (24)$$

$$\rho_b\left[\frac{\partial T}{\partial t}+u_b\frac{\partial T}{\partial x}+v\frac{dT_b}{dy}\right]=(\gamma-1)M_\infty^2\left[\frac{\partial p}{\partial t}+u_b\frac{\partial p}{\partial x}+\frac{1}{R}\phi\right]$$
$$+\frac{1}{R\,Pr}\left\{\mu_b\frac{\partial^2 T}{\partial x^2}+\frac{\partial}{\partial y}\left(\mu_b\frac{\partial T}{\partial y}+\mu\frac{dT_b}{dy}\right)+\mu_b\frac{\partial^2 T}{\partial z^2}\right\} \qquad (25)$$

$$\phi=2\mu_b\left(\frac{\partial u}{\partial y}+\frac{\partial v}{\partial x}\right)\frac{du_b}{dy}+\mu\left(\frac{du_b}{dy}\right)^2 \qquad (26)$$

where

$$r=\frac{2}{3}(e+2) \quad \text{and} \quad m=\frac{2}{3}(e-1) \qquad (27)$$

and e = 0 corresponds to the Stokes hypothesis. The local Reynolds number R in Equations 21-26 is based on a reference length ($\delta_r^* = \sqrt{\nu^* x_r^* / U_\infty^*}$), which is the order of the boundary layer thickness where $x^*_r$ is the distance from the leading edge to the location where the calculations are

performed. Velocities are normalized with respect to the freestream velocity ($U^*_\infty$) and lengths are normalized with respect to ($\delta^*_r$) Hence,

$$R=\frac{U^*_\infty \delta^*_r}{\nu^*}=\sqrt{\frac{U^*_\infty x^*_r}{\nu^*}} \qquad (28)$$

The boundary conditions at the wall are:

$$u = v = W = T = 0 \text{ at } Y = 0 \qquad (29)$$

For sonic, subsonic and supersonic waves the boundary conditions away from the wall have the general form[11]:

u, v, w, T, p, are bounded as $y\to\infty$ (30)

We assume that $\mu$ is only a function of the temperature, hence

$$\mu = T\frac{d\mu_b}{dT}(T_b) = T\mu'_b(T_b) \qquad (31)$$

Moreover, the linearized equation of state takes the form

$$p/p_b T/T_b+\rho/\rho_b \qquad (32)$$

Because the mean flow is assumed to be quasi-parallel, we seek a solution of Equations 21-25, 26, 27, and 29 in the form of 3D traveling Tollmien-Schlichting waves as

$$[u, v, p, T, w] = [\zeta_1(y), \zeta_3(y), \zeta_4(y), \zeta_5(y), \zeta_7(y)]^* \exp\left[i\left(\int \alpha dx + \beta z - \omega t\right)\right] \qquad (33)$$

where $\alpha$, and $\beta$ are the streamwise and spanwise wave numbers, respectively, and $\omega$ is the frequency. Substituting Equations 30-32 into Equations. 21-25, we obtain

$$D\zeta_3 + i\alpha\zeta_1 - \frac{DT_b}{T_b}\zeta_3 + i(\alpha u_b - \omega)^* (\gamma M^2_\infty \zeta_4 - \frac{\xi_5}{T_b}) + i\beta\zeta_7 = 0 \qquad (34)$$

$$i(\alpha u_b - \omega)\zeta_1 + \zeta_3 Du_b + i\alpha T_b\zeta_4 - \frac{T_b}{R}\{-\mu_b(r\alpha^2+\beta^2)\zeta_1 - \alpha\beta\mu_b(m+1)\zeta_7 + i(m+1)\alpha\mu_b D\zeta_3 + \mu'_b D\zeta_1 + i\alpha\mu'_b\zeta_3 + \mu_b D^2\zeta_1 + D(\mu'_b Du_b)\zeta_5 + \mu'_b Du_b D\zeta_5\} = 0 \qquad (35)$$

$$i(\alpha u_b - \omega)\zeta_3 + T_b D\zeta_4 - \frac{T_b}{R}\{i(m+1)\alpha\mu_b D\zeta_1 + im\alpha\mu'_b\zeta_1 - (\alpha^2+\beta^2)\mu_b\zeta_3 + r\mu'_b D\zeta_3 + im\beta\mu'_b\zeta_7 + i\alpha\mu'_b Du_b\zeta_5 + r\mu_b D^2\zeta_3 + i(m+1)\beta\mu_b D\zeta_7\} = 0 \qquad (36)$$

$$i(\alpha u_b - \omega)\zeta_7 + i\beta T_b\zeta_4 - \frac{T_b}{R}\{-(m+1)\alpha\beta\mu_b\zeta_1 + i\beta\mu'_b\zeta_3 + i(m+1)\beta D\zeta_3 - \mu_b(\alpha^2+r\beta^2)\zeta_7 + \mu'_b D\zeta_7 \mu_b D^2\zeta_7\} = 0 \qquad (37)$$

$$i(\alpha u_b - \omega)\zeta_5 + \zeta_3 DT_b - i(\gamma-1)T_b M^2_\infty(\alpha u_b - \omega)\zeta_4 - \frac{T_b}{R}[2Du_b(D\zeta_1 + i\alpha\zeta_3) + \mu'_b(Du_b)\zeta_5] - \frac{T_b}{RPr}[-\mu_b(\alpha^2+\beta^2)\zeta_5 + D(\mu_b D\zeta_5) + D(\mu'_b DT_b\zeta_5)] = 0 \qquad (38)$$

$$\zeta_1 = \zeta_3 = \zeta_5 = \zeta_7 = 0 \text{ at } y = 0 \qquad (39)$$

$\zeta_n$ are bounded as $y \to \infty$ (40)

where the prime denotes the derivatives with respect to the argument and D = d/dy

In this work, we consider the case of spatial stability so that $\omega$ is real. Because the basic flow is two-dimensional,$\beta$ is constant, and we assume that $\beta$ is real and $\alpha$ is complex so that

$$\alpha=\alpha_r+i\alpha_I \qquad (41)$$

moreover, we compute $\omega$ from the non dimensional frequency F as

$$\omega = RF \qquad (42)$$

and we also compute the wave angle $\Psi$ as

$$\psi = \tan^{-1}(\beta/\alpha_r) \qquad (43)$$

The eigenvalue problem is solved by using the finite-difference code BVPFD [13] coupled with the Newton-Raphson iteration technique. This scheme produces results that are as accurate as those obtained by using SUPORT [14] with far less computational effort. The analysis presented here is valid for parallel flows, however, for non-parallel flows one can use the parabolized stability equation analysis (P.S.E) [19].

## RESULTS AND DISCUSSION

After Calculating the mean flow and for a chosen F, R and $\psi$ we calculate the growth rates at the profile and then we march in the x direction to calculate the growth rates at adjacent stations. We present results for second-mode instability waves, and since it has higher growth rates than the first mode, it is more crucial for transition at the investigated Mach number.

As mentioned earlier Malik [12] attempted to investigate the effect of pressure gradient on the stability of supersonic boundary layer. However, he, mistakenly, used the self-similar velocity profile for Pr = 0.70 by neglecting the left-hand-side of Equations 10,11. We reproduced his calculations with a good accuracy when using a self-similar velocity profile. Figure 1 shows the effect of $\beta_o$ on the second-mode growth rates of a 4.5 Mach flow at R = 1500 , Pr = 0.72 and wind tunnel temperature using self-similar calculations. As it is clear a positive value of $\beta_o$ of 0.025 is not sufficient to stabilize the flow. In Figure 2, however, we show the growth rates for the same flow conditions but this time we used the non-similar boundary layer calculations. It is obvious That a value of $\beta_o$ of 0.025 is sufficient to totally stabilize the flow at the Reynolds numbers. Hence, using the self-similar calculations, although considerably reduce calculations effort, it results in an inaccurate calculations of the growth rates, since the growth rates are quite sensitive to the accuracy of the mean flow. By marching downstream the effect of pressure gradient on the second-mode-waves growth rates is shown in Figure 3. Not only the growth rates decrease as $\beta_o$ increases, but the critical Reynolds number also increases, hence a delaying transition further downstream.

Although for incompressible flows a constant $\beta_o$ represent a flow over a wedge, it is not the case for supersonic flows. In fact that type of flow does not represent a flow over a simple geometry. The dependence of $U_e$ on X is rather complicated as demonstrated by Equation 15-a. In Figure 4 we compare the growth rates between simply retarded, simply accelerated, and constant $U_e$ flows at 4.5 Mach. As the flow accelerates it becomes more stable and the critical R shifts downstream hence delaying transition .

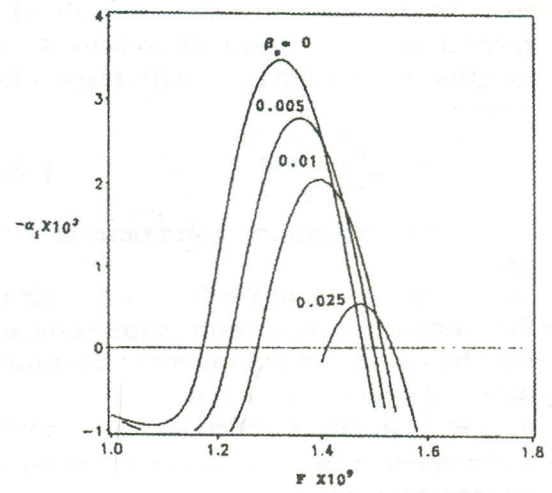


***Figure 1*** Growth rate versus frequency for various $\beta_o$.self similar assumption, R=1500, Pr=0.72, $M_\infty$=4.5, and $T_\infty$ =121 K.

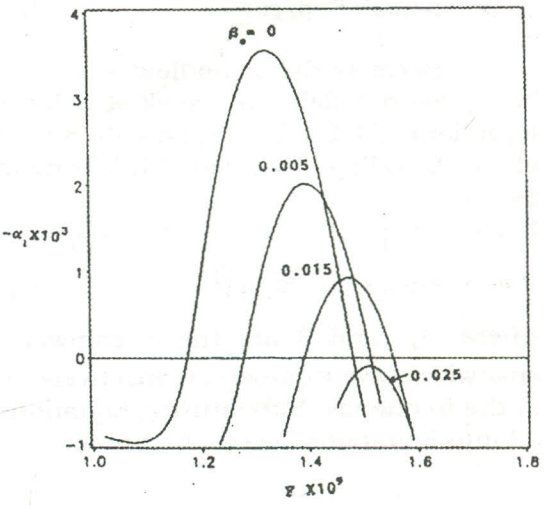


***Figure 2*** Growth rate versus freqency for various $\beta_o$. Non-similar assumption, R=1500, Pr=0.72, $M_\infty$=4.5, and $T_\infty$=121 K.

On the other hand decelerating the flow does not only increase the growth rates, it also decreases the critical R and hence advancing transition upstream.

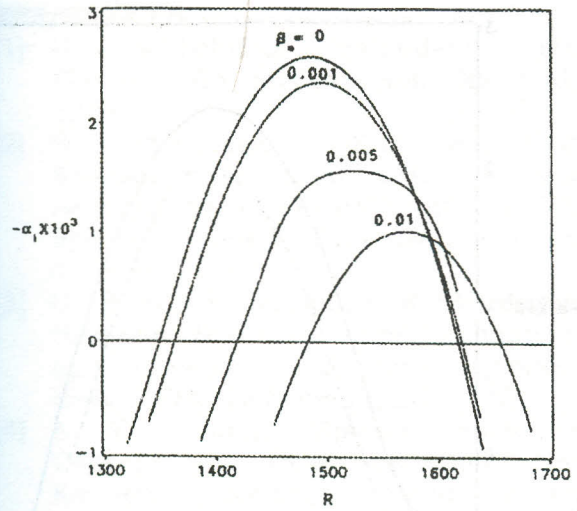


*Figure 3* Growth rate versus frequency for various $\beta_o$. Non-similar calcuations, Pr=0.72, $M_\infty$=4.5, $T_\infty$=121 K, and F = 5x10$^{-6}$.

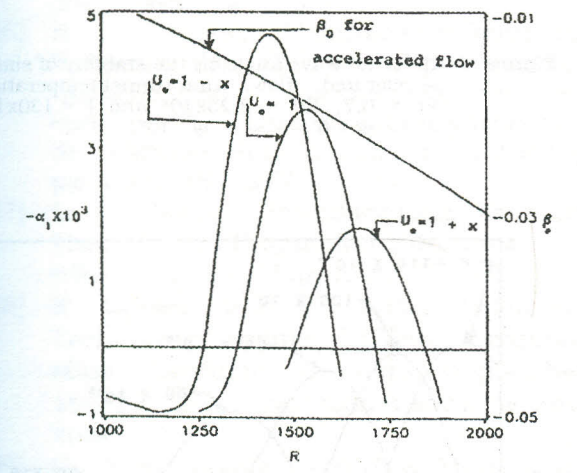


*Figure 4* Growth rate versus R for simply retarded, simply accelerated, and zero pressure gradient flows. Non similar calculations, Pr=0.72, $M_\infty$=4.5, wind tunnel temperature, Re = 2.25x10$^8$ and F = 130x10$^{-6}$.

For that type of flow $\beta_0$ is not constant and it varies with X as described in Equation 14-b. Figure 4 also shows the variation of $\beta_0$ for the retarded flow with R. It is clear that $\beta_0$ decreases (becomes more negative) as marching downstream.

## ERROR ANALYSIS

In the mean flow analysis the minimum stepsize in the $\eta$ direction is 0.01, while its value equals 0.05 in the x-direction. The accuracy in calculating the eigen value is (1+i)x10$^{-6}$, while the normalized error in the eigen function is 10$^{-14}$. For adiabatic flow over flat plate we compared our calculations of $\alpha$ with that of Mack [10,11] and the agreement was up to the sixth digit. As such no numerical instability is expected in our analysis.

## CONCLUSIONS

It is found that increasing $M_\infty$ seems to have a destabilizing effect on the accelerated flow as shown in Figure 5. For the same frequency the growth rates are considerably increased as the Mach number increases from 4.5 to 5.0. Moreover, the critical R shifts considerably upstream enhancing an earlier transition. suprisingly it is the other way around for the retarded flow. Figure 6 shows that as $M_\infty$ increases from 4.5 to 5.0 the growth rates decreases. However, the trend of decreasing the critical R still exists for retarded flows.

As shown in Figure 7 the most unstable mode is still the two-dimensional one, and for all R. Pressure gradient on the other hand, doesn't affect the wave angle of the most unstable second-mode waves. Figure 8 shows the variation of the growth rates with R for different frequencies, it is clear that the most dangerous frequencies are the relatively high once.

## ACKNOWLEDGMENT

The authors would like to thank Prof. A. H. Nayfeh for his help and for facilitating the use of the computer facility at VPI and SU, VA, U.S.A.

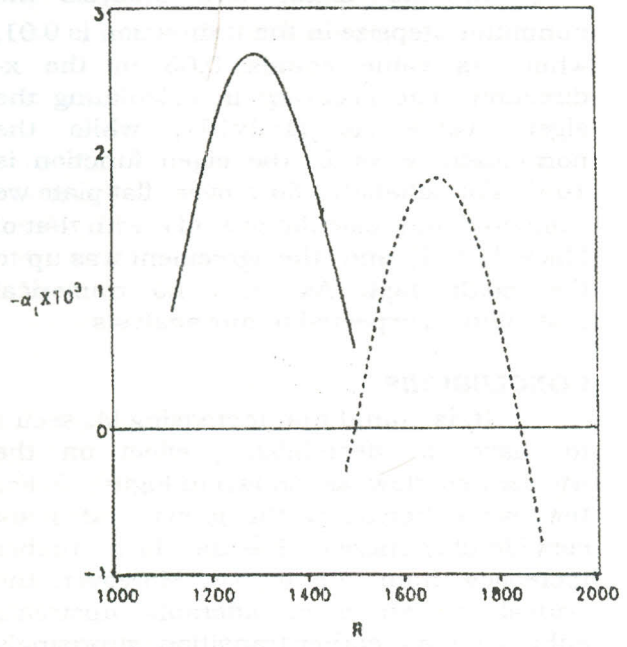


***Figure 5*** Effect of Mach number on the stability of simply accelerated flow, wind tunnel temperature, Pr = 0.7, Re = $2.25x10^8$ and F = $130x10^{-6}$. ——— $M_\infty$=5, ---- $M_\infty$ = 4.5.

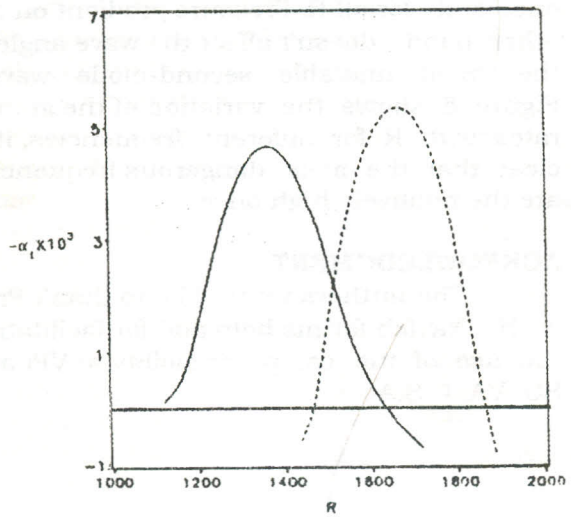


***Figure 6*** Effect of Mach number on the stability of simply retarded flow, wind tunnel temperature, Pr = 0.7, Re = $2.25x10^8$ and F = $130x10^{-6}$. ——— $M_\infty$ = 4.5, ------ $M_\infty$ = 5.

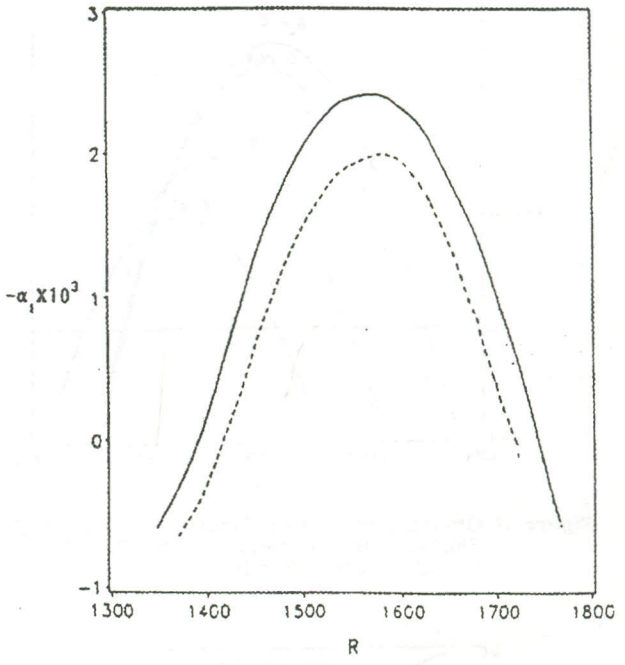


***Figure 7*** Effect of wave angle on the stability of simply accelerated flow, wind tunnel temperature, Pr = 0.7, Re = $2.25x10^8$, and F = $130x10^6$. ——— $\psi = 0^\circ$, -------- $\psi = 10^\circ$.

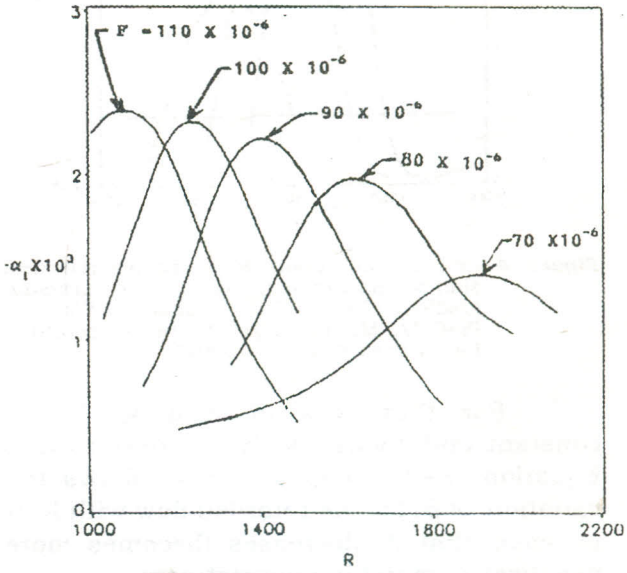


***Figure 8.*** Effect of frequency on the stability of simply accelerated flow, wind tunnel temperature, Pr = 0.7, and Re=$2.25x10^8$.

**REFERENCES**


[1] H. Schlichring, "Boundary Layer Theory," Co. McGraw-Hill, New York, 1979.

[2] W. Pfenninger, "USAF and Navy Sponsored Northrop LFC Research Between 1949 and 1967, "AGARD/VKI Special Course for Drag Reduction. pp. 3.1-3.75,1977.

[3] G. B Schubauer, and H. K. Skarmstad, "Laminar Boundary Layer Oscillations and Transition on a Flat Plate," NASA Report 909, Washington, DC. 1948.

[4] A. D. Young, "Special Course on Concepts for Drag Reduction," Von Karmen Institute, Rhode-Genese, Belgium, AGARD-R654, 1977

[5] R. E. Kosin, "Laminar Flow Control By Suction as Applied to the X-21 Airplane," J. Aircraft, Vol. 2, pp.384-390, 1965.

[6] R. T. Witcomb, "Methods for Reducing Subsonic Drag Due to lift," presented at AGARD/VjKi, Special course on concepts for Drag Reduction, Rhodes - St. Genese, Belgium, March 28-April 1, pp. 2.1-2.38, 1977.

[7] L. M., Mack "Boundary Layer Stability Theory", Jet Propulsion Lab. Document 900-277(rev. A), Pasadena, Ca, 1969.

[8] R. Eppler, and H. Fasel, "Laminar-Turbulent-Transition,"IUTAM Symposium, Stuttgart, Germany, September 16-22. 1979, Springer-Verlag , New York, 1980.

[9] G. B. Schubauer, and H. K. Skarmstad, "Laminar Boundary Layer Oscillations and Transition on a Flat Plat," J. Aero. Sci. Vol. 14, pp.69-73, 1947.

[10] L. M. Mack, "Transition Reduction and Linear Stability Theory," AGARD CP-224, Denmark, 1977.

[11] L. M. Mack, "Stability of Compressible Laminar Boundary Layer According to a Direct Numerical Solution," AGARD 97, Part I, pp.329-345, 1965.

[12] R. M. Malik, "Prediction and Control of Transition in Hypersonic boundary Layers," AIAA Paper No. 87-1414, June, 1987.

[13] V. Pereyra, "PASAV3: An Adaptive Finite Difference FORTRAN Program for First Order Nonlinear, Ordinary Boundary Value problem, in Lecture Notes in Computer Science, edited by B. Childs, M. Scott, J. Daniel, E. Denman, and P. Nelson, Springer, Berlin, pp. 67-88, 1976.

[14] M. R. Scott, and A. H. Watts, "Computational Solution of Linear Two-Points Boundary Value Problems Via Orthonormalization," SIAM, J. Num. Anal. Vol. 14, pp.40-70, 1977.

[15] A. A. Al-Maaitah, A. H. Nayfeh, and Massad, J. A., " Effect of Suction on the Stability of Compressible Boundary-Layers; I. Second-Mode Waves," J. of Fluids Engineering (ASME) Vol. 113, No. 4, pp. 591-596,1991.

[16] J. A. Massad, A. H. Nayfeh, and A. A. Al-Maaitah, " Effect of Suction on the Stability of Compressible Boundary-Layers; II. First-Mode Waves," J. of Fluid Engineering (ASME) Vol. 113, No.4, pp. 597-602,1991.

[17] J.A. Massad, A. H. Nayfeh, and A.A Al-Maaitah, "Effect of Heat Transfer on the Stability of Bondary-Layer," J. of Computers and Fluids, Vol. 21, No. 1, pp.43-61, 1992

[18] A.A. Al-Maaitah, A.H. Nayfeh, and S.A. Rageb, " Effect of Cooling on the Stability of Compressible Subsonic Flows over Smooth Humps and Backward-Facing Steps," Phys. Fluids A, Vol. 2, No. 3, pp. 381-389, 1990

[19] M. Malik, "Parapolized Stability Equation for Compressible and Incompressible Boundary Layer", in proceedings of first bombardier International Workshop Monterial, Canada, 1993,

[20] A. Michalle, and A. Al-Maaitah, " On the Receptivity of the Unstable Wall Boundary Layer Along a Surface Hump Excited by a 2-Dirace Source and the Wall," European. Jornal of Mechanics B: Fluids, Vol. 11, No. 5, pp. 521-546,1992.